Supplement of Solid Earth, 13, 117–136, 2022
https://doi.org/10.5194/se-13-117-2022-supplement

Solid Earth
Open Access

Supplement of

Forearc density structure of the overriding plate in the northern area of the giant 1960 Valdivia earthquake

Andrei Maksymowicz et al.

Correspondence to: Andrei Maksymowicz (andrei.maksymowicz@uchile.cl)

S1 Location of Electromagnetic soundings

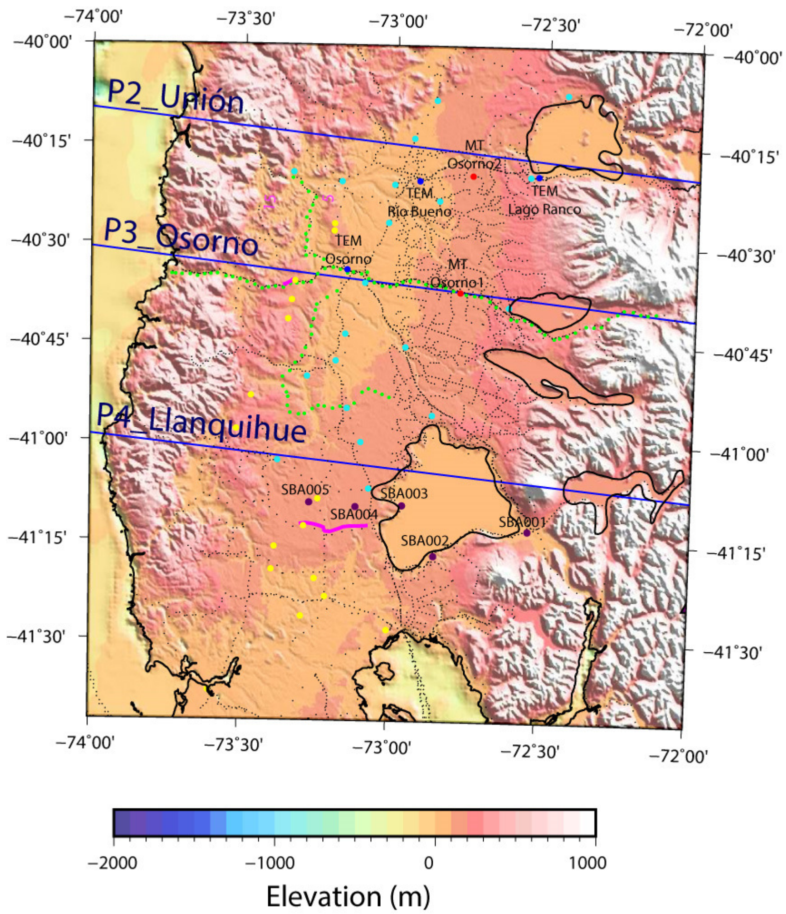

Figure S1.1: Location of MT and TEM data in the study zone. The blue and red dots correspond to TEM soundings and MT stations acquired under the aforementioned FONDECYT project. Magenta dots indicate the MT stations presented by Segovia et al. (2021) and cyan dots correspond to TEM soundings published by DGA (2012). The blue lines indicate the location of regional density model. The black dots designate gravity stations compiled by Schmidt and Götze (2006), onshore, and in GEODAS database (NOAA) offshore. The green dots illustrate the complementary gravity stations acquired by our group under the ANID-FONDECYT project Nº11170047. Seismic reflection lines presented by Jordan et al. (2001) indicated with magenta lines. The yellow dots correspond to the location of boreholes (McDonough et al., 1997).

S2 Magnetotelluric Models

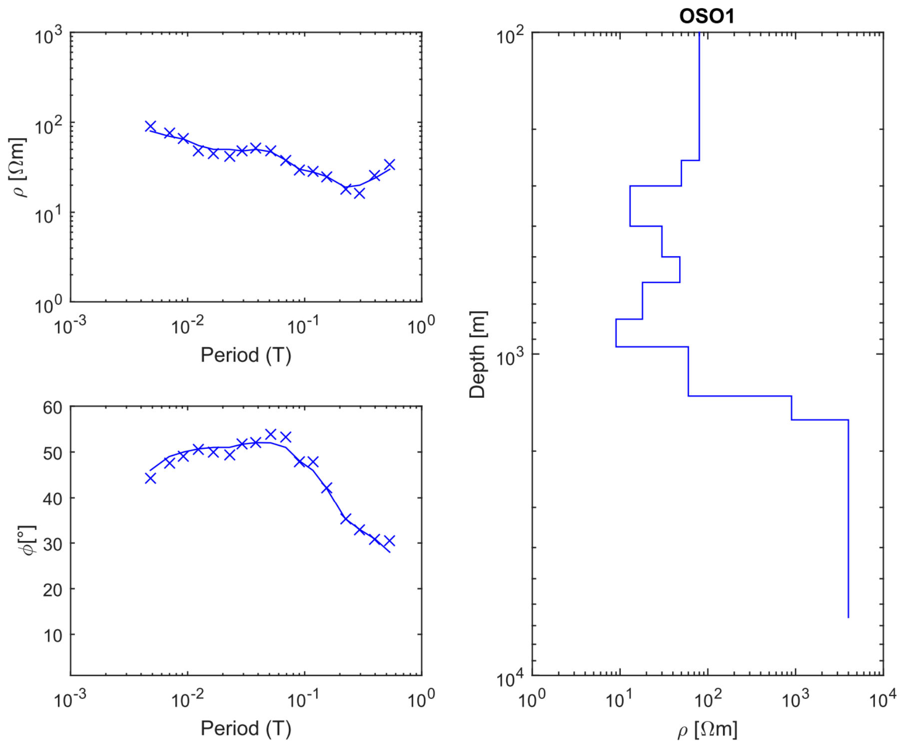

Figure S2.1: MT data (crosses) and corresponding 1D resistivity depth model (blue lines) at station Osorno 1.

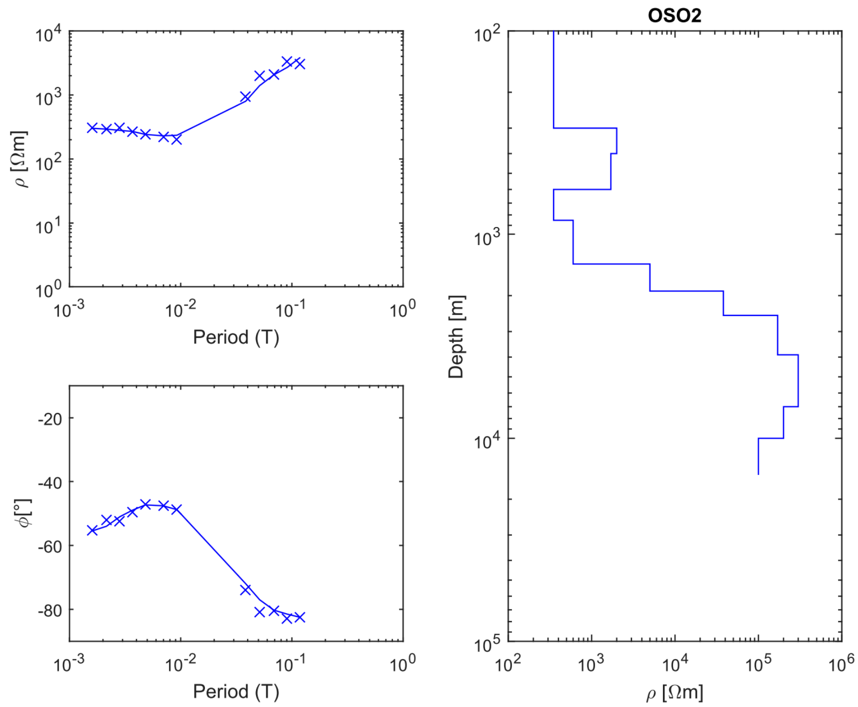

Figure S2.2: MT data (crosses) and corresponding 1D resistivity depth model (blue lines) at station Osorno 2.

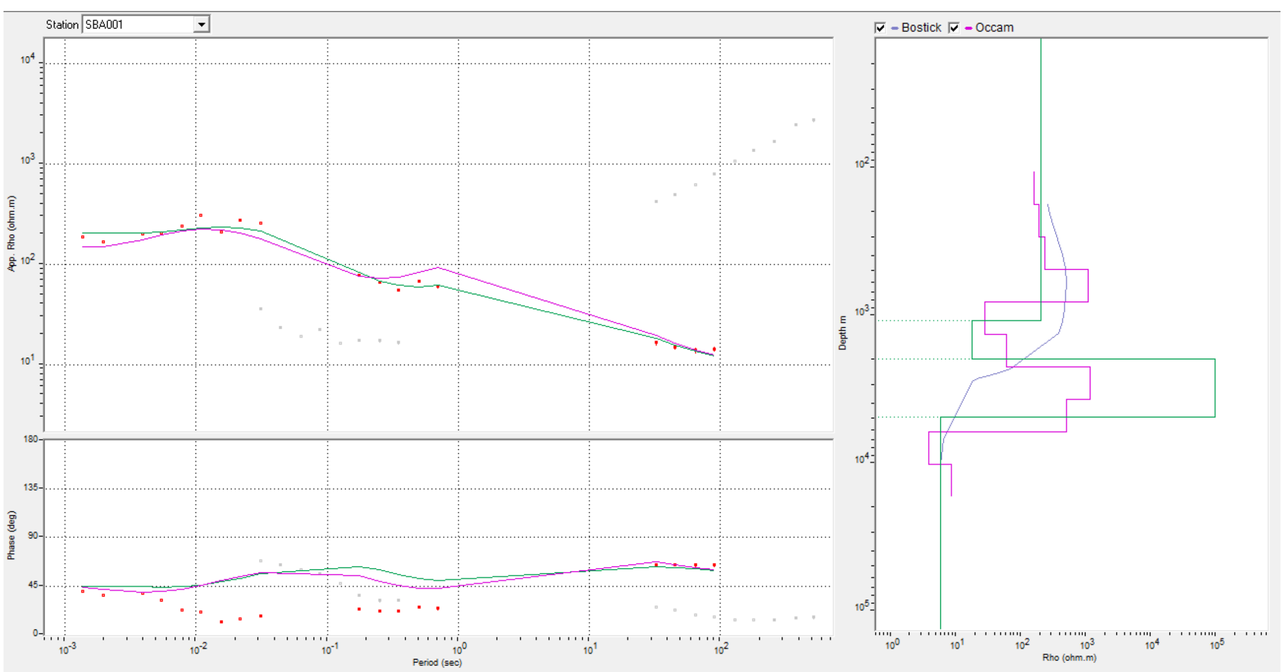

Figure S2.3: MT data (red dots) and corresponding 1D resistivity depth model (lines) at station SBA001.

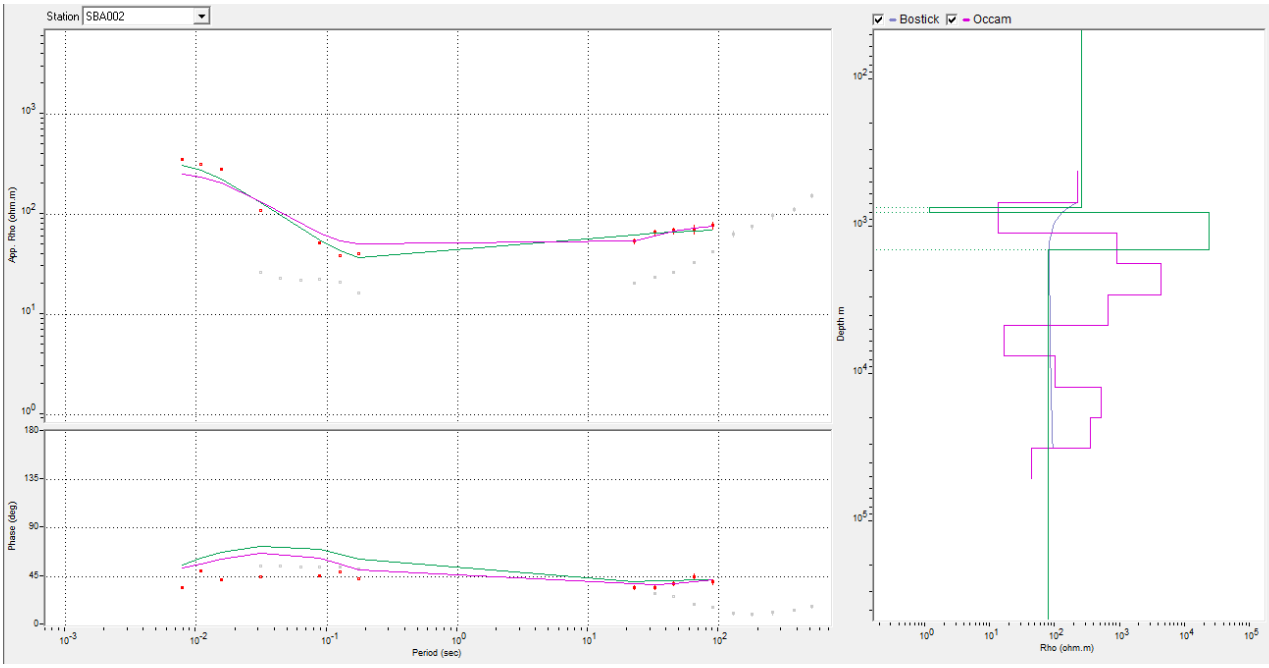

Figure S2.4: MT data (red dots) and corresponding 1D resistivity depth model (lines) at station SBA002.

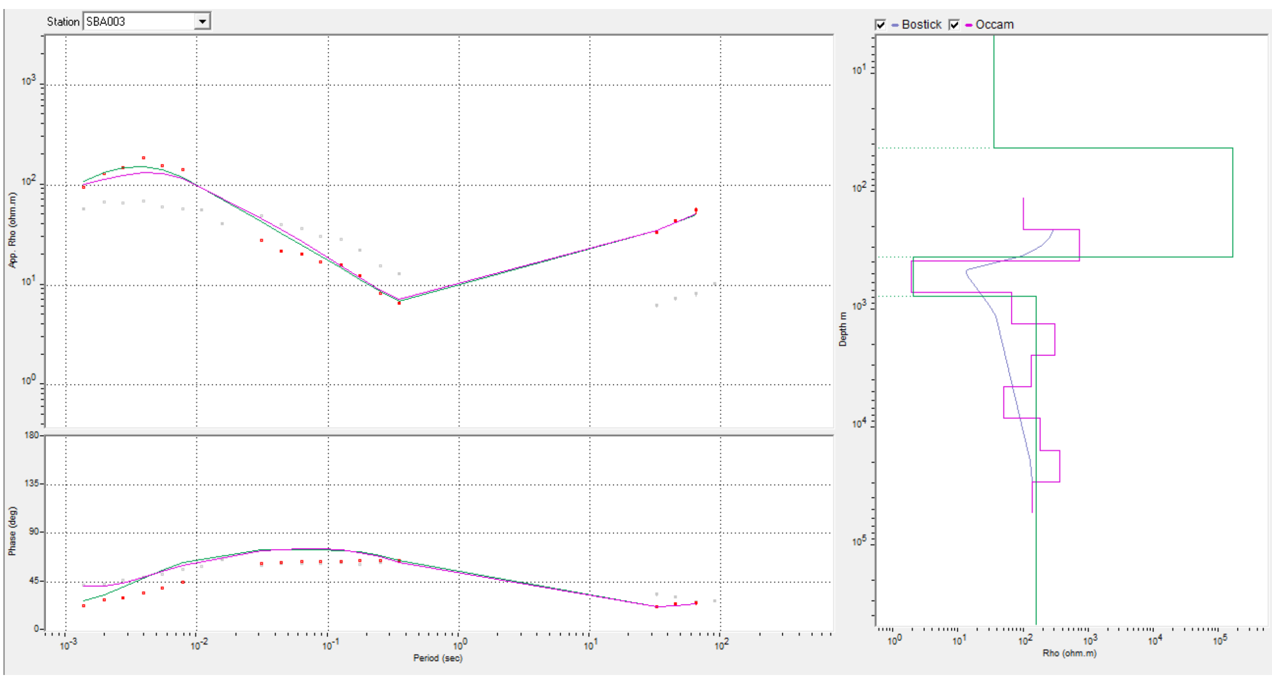

Figure S2.5: MT data (red dots) and corresponding 1D resistivity depth model (lines) at station SBA003.

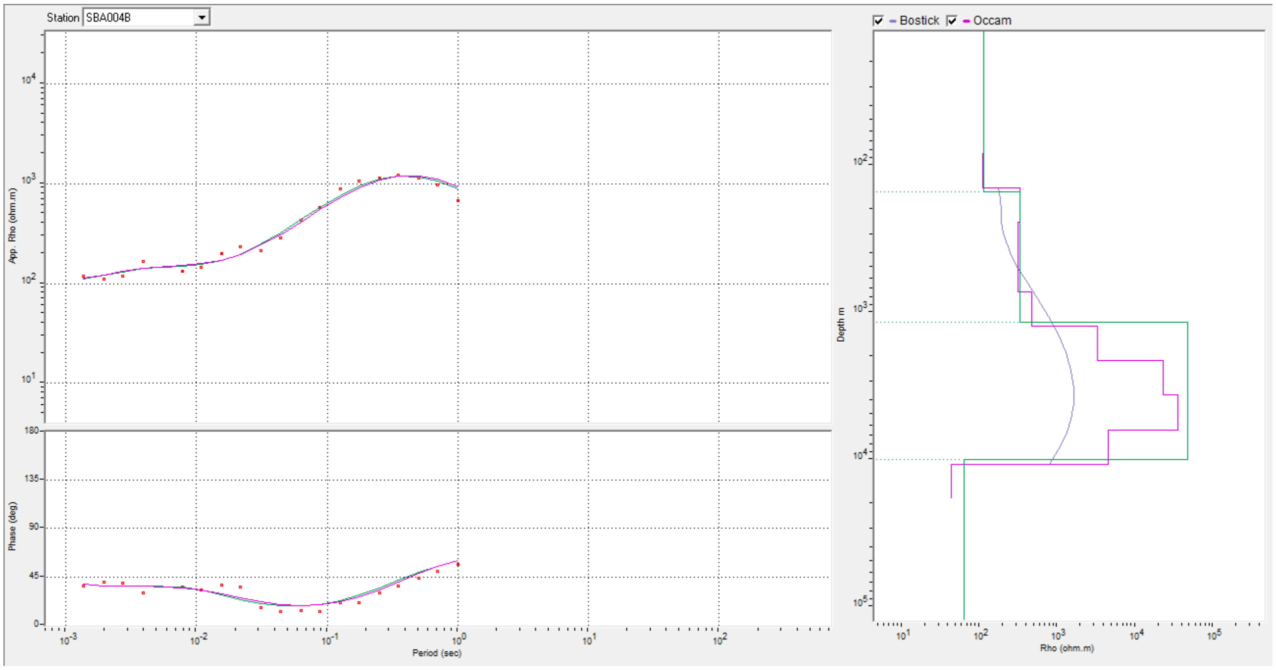

Figure S2.6: MT data (red dots) and corresponding 1D resistivity depth model (lines) at station SBA004.

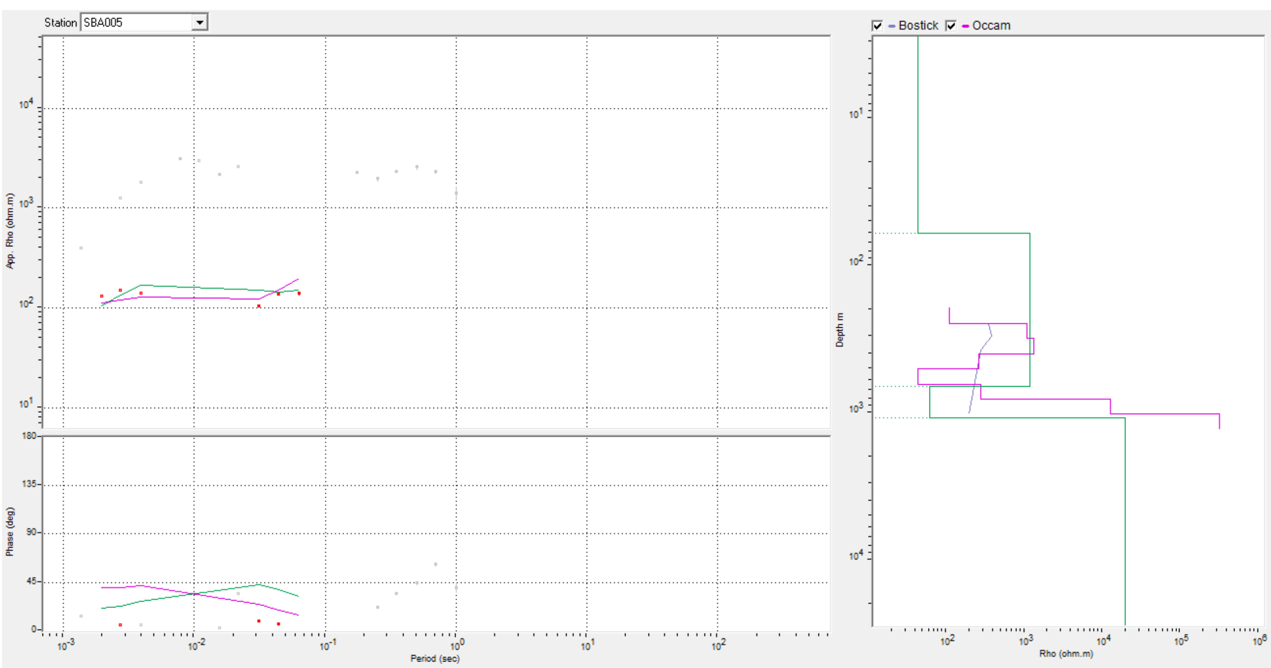

Figure S2.7: MT data (red dots) and corresponding 1D resistivity depth model (lines) at station SBA005.

3 Transient electromagnetics models

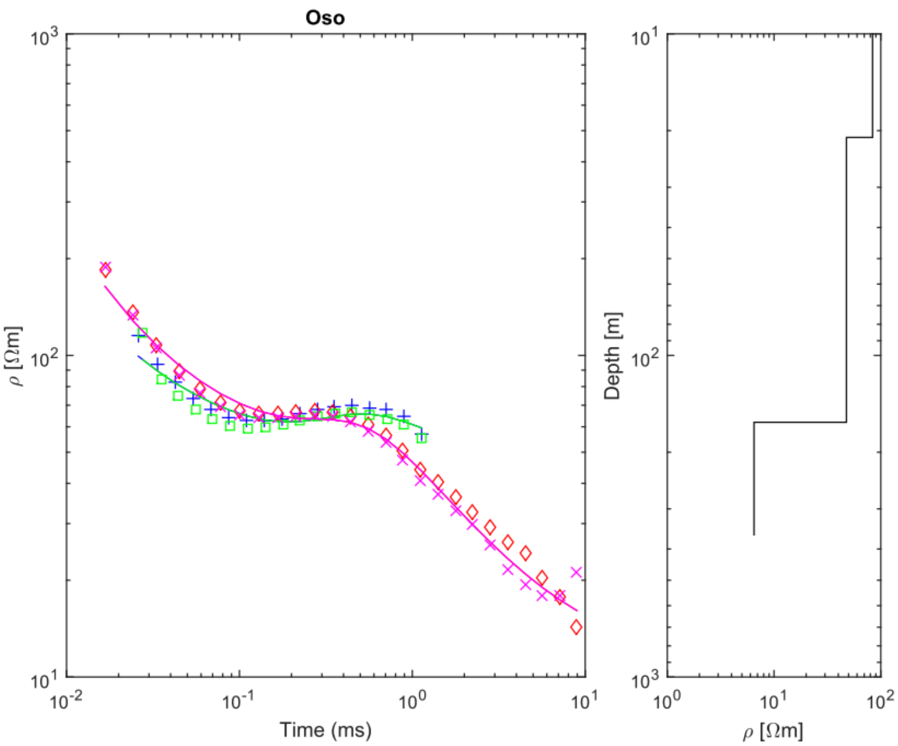

Figure S3.1: TEM data (symbols) and corresponding 1D resistivity depth model (lines) at station TEM Osorno.

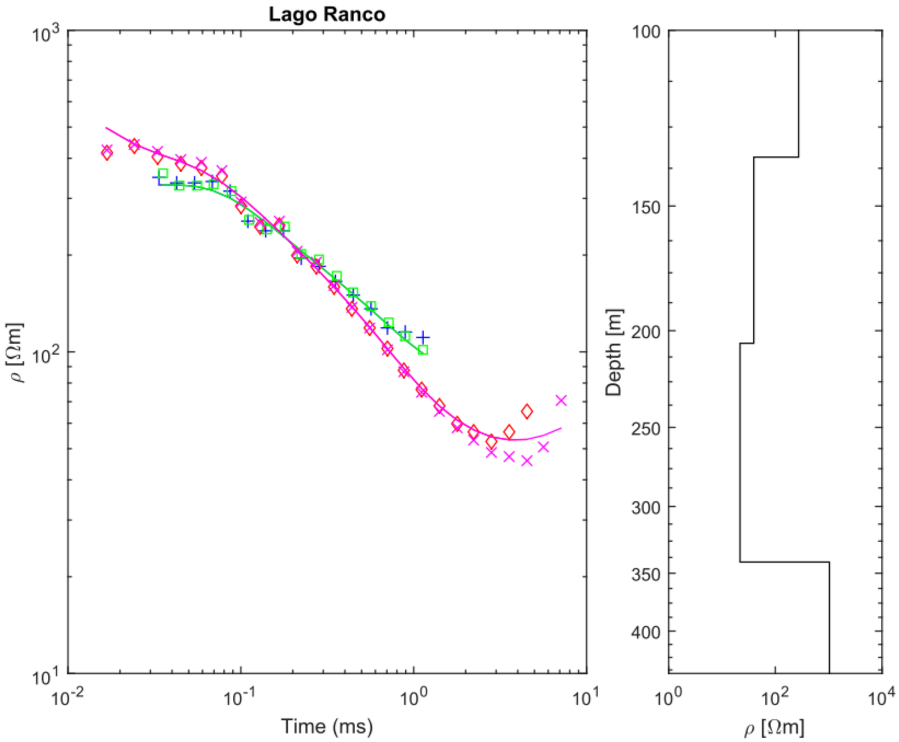

Figure S3.2: TEM data (symbols) and corresponding 1D resistivity depth model (lines) at station TEM Lago Ranco.

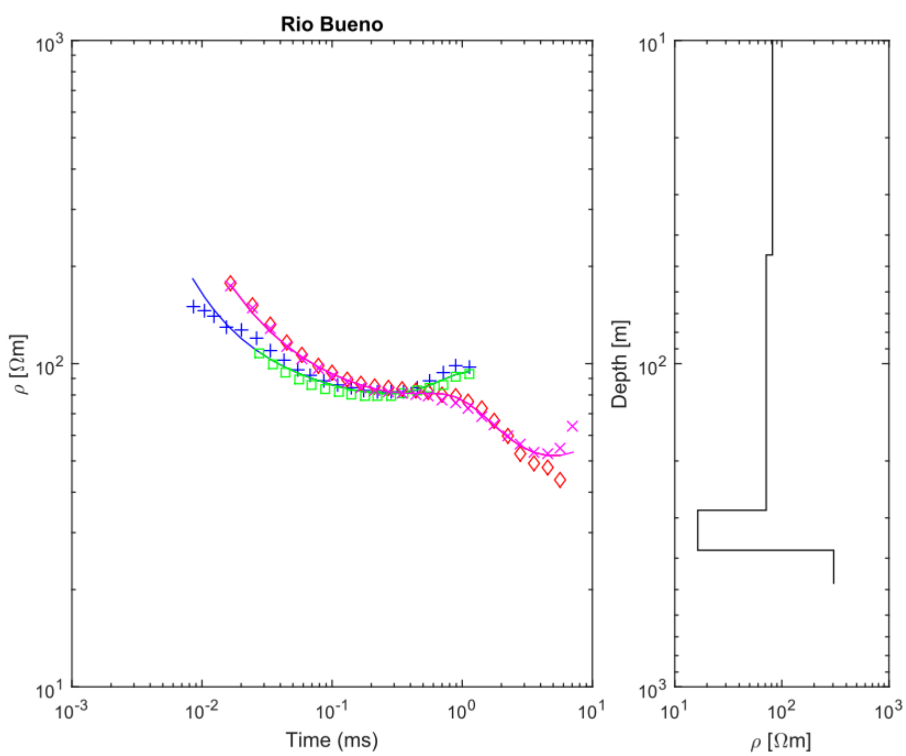

Figure S3.3: TEM data (symbols) and corresponding 1D resistivity depth model (lines) at station TEM Rio Bueno.

4 Regional gravity lineaments and derivative filters

The regional gravity lineaments, presented in the main text, were visually interpreted. Similar qualitative exercise is often used in bathymetric/topographic analysis, potential fields data and other geophysical/geological studies to highlight linear features in the signal that could be related (or not) with hidden structures and other geological features at depth. To make easier this qualitative interpretation, it is a common practice to generate set of derivative filters of the original signal to highlight short wavelength features. However, it is worth noting that these filters increase the noise/signal ratio, which in some cases could make difficult their interpretation. For this reason, it is necessary to keep in sight the original data as a primary source for qualitative interpretation. Figure S4.1 present the interpreted lineaments and maps of the CBA filtered by: first derivative to the west (dg/dx), first derivative to the north (dg/dy), directional derivative to the northeast (azimuth=45º), slope gradient ($\sqrt{(\mathrm{dg}/\mathrm{dx})^2 + (\mathrm{dg}/\mathrm{dy})^2}$) and analytical signal ($\sqrt{(\mathrm{dg}/\mathrm{dx})^2 + (\mathrm{dg}/\mathrm{dy})^2 + (\mathrm{dg}/\mathrm{dz})^2}$)
Derivative filters were generated using the standard procedure in frequency domain (Blakely, 1995).

Blakely, R.J. (1995) Potential Theory in Gravity & Magnetic Applications. Cambridge University Press, Cambridge. http://dx.doi.org/10.1017/CBO9780511549816

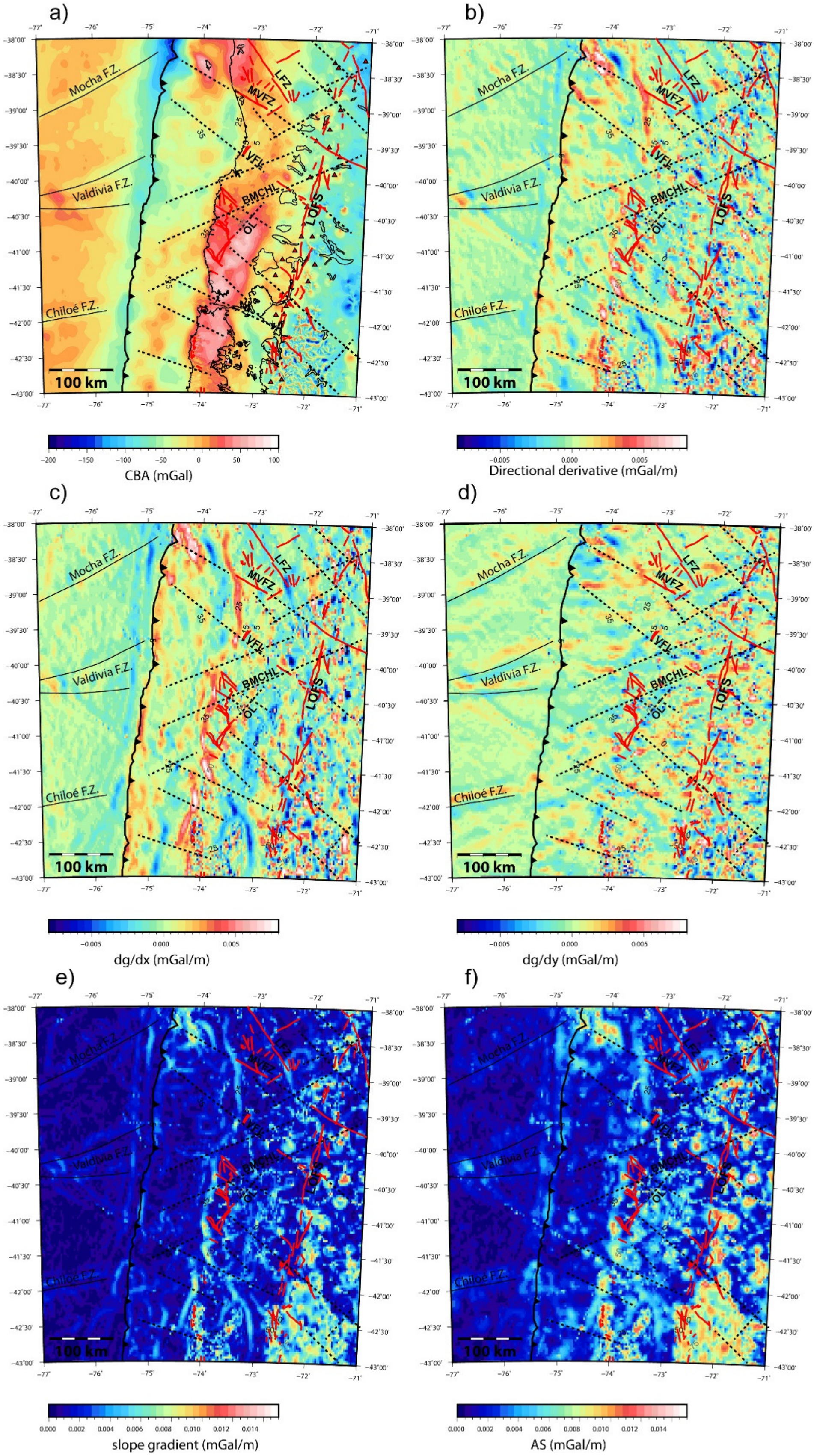
a)
b)
c)
d)
e)
f)
Mocha F.Z.
Valdivia F.Z.
Chiloé F.Z.
LFZ
MVFZ
VFL
BMCHL
OL
LOFS
100 km
CBA (mGal)
Directional derivative (mGal/m)
dg/dx (mGal/m)
dg/dy (mGal/m)
slope gradient (mGal/m)
AS (mGal/m)

Figure S4.1: Interpreted gravity lineaments and derivative filters of CBA. Dotted black lines are interpreted gravimetric lineaments, e.g., Valdivia-Futrono lineament (VFL), Bahía Mansa-Choshuenco lineament (BMCHL) and Osorno lineament (OL). Red lines correspond to continental structures identified at the surface (SERNAGEOMIN, 2003; Melnick and Echtler, 2006), including: Liquiñe-Ofqui fault system (LOFS), Mocha-Villarrica fault zone (MVFZ) and Lanalhue fault zone (LFZ). The red triangles illustrate active volcanoes. a) Interpreted gravity lineaments and CBA signal. b) Interpreted gravity lineaments and the directional derivative of CBA to the northwest (azimuth=45º). c) Interpreted gravity lineaments and the first derivative of CBA to the west (dg/dx). d) c) Interpreted gravity lineaments and the first derivative of CBA to the north (dg/dy). e) Interpreted gravity lineaments and the slope gradient of CBA. f) Interpreted gravity lineaments and the analytical signal of CBA.

S5 2D Forward models

Below we show individual figures for each of 5 2D profiles presented in Fig. 4 of the main text.

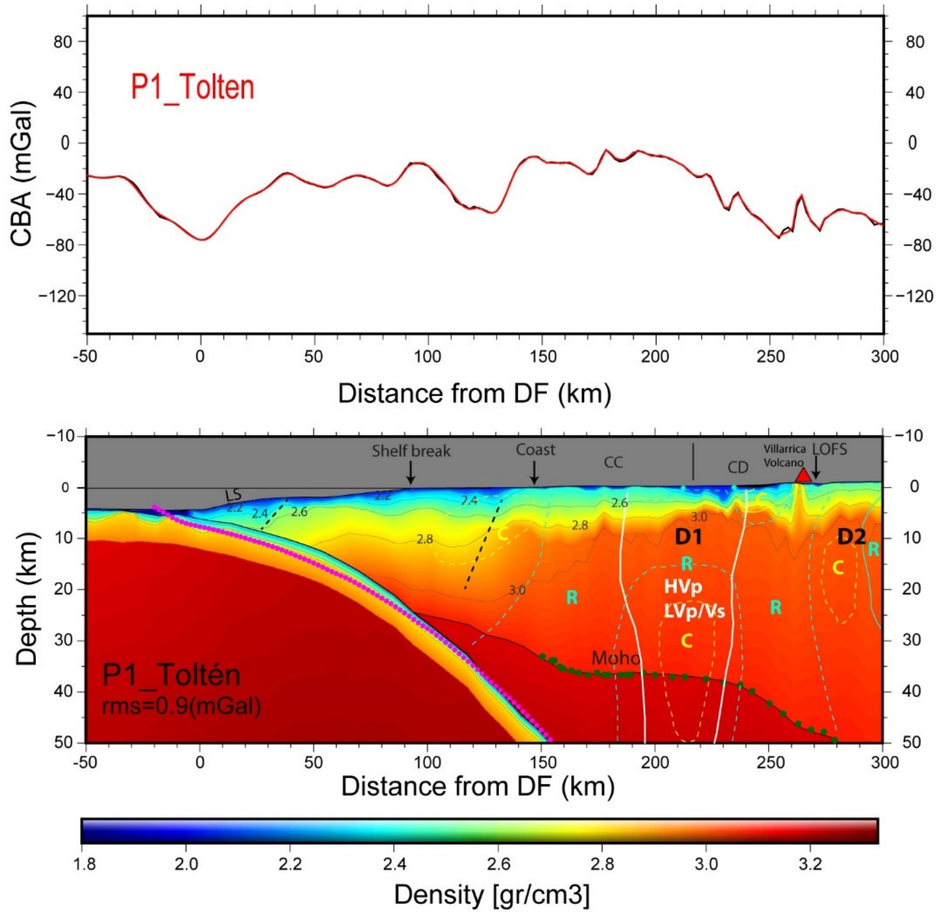

Figure S5.1: 2D regional forward model at profile P1_Toltén. Upper panel shows the observed Complete Bouguer Anomaly (CBA) in black and the calculated curve in red. Lower panel present the corresponding density depth model. Morphological limits of the continental wedge (as lower slope, LS) are indicated. Dotted black lines illustrate the approximate limits of frontal low density unit and the middle wedge/shelf unit of the marine continental wedge. Thin vertical line indicates the limit between CC and CD. Red triangles correspond to the active volcanoes located near the profile. Pink dots correspond to slab geometry according to SLAB2.0 model (Hayes et al., 2018). Green dots depict the continental Moho depths obtained by receiver functions analysis (Dzierma et al., 2012a). Cyan dots correspond to minimum thickness of this sedimentary layer according to MT and TEM soundings. White lines limit a zone of high Vp and low Vp/Vs obtained by Dzierma et al. (2012b). Thin dotted yellow and cyan lines limit electrical conductive and resistive zones (C and R) according to Kapinos et al. (2016).

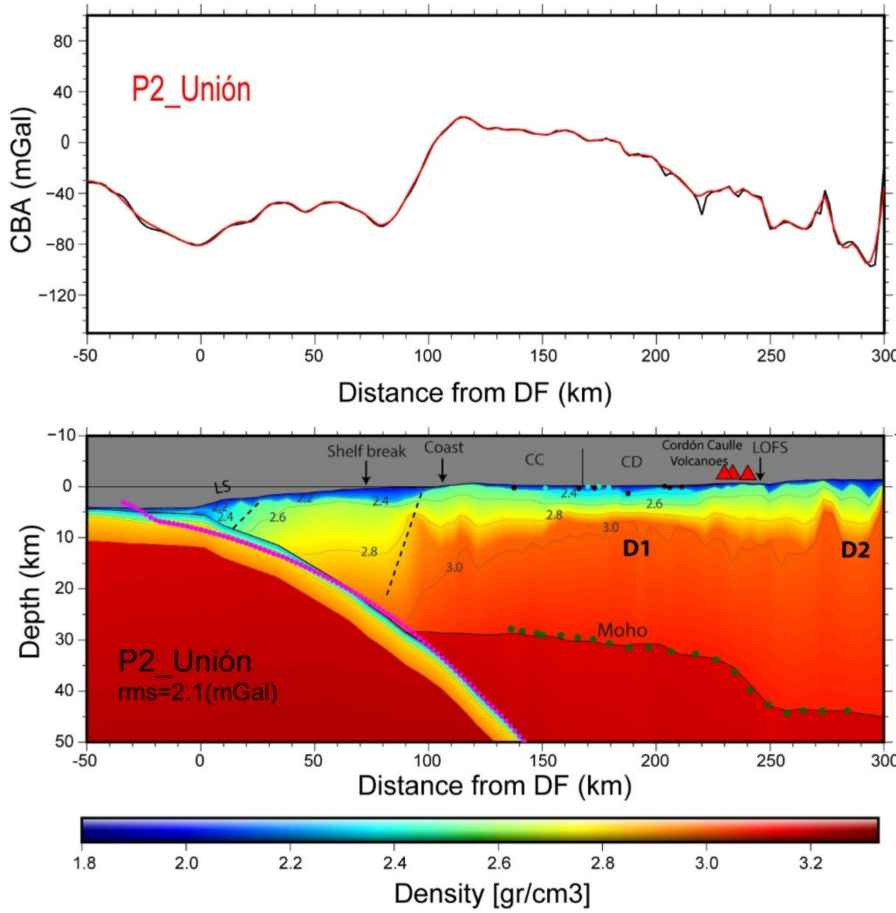

Figure S5.2: 2D regional forward model at profile P2_Unión. Upper panel shows the observed Complete Bouguer Anomaly (CBA) in black and the calculated curve in red. Lower panel present the corresponding density depth model, morphological limits of the continental wedge (as lower slope, LS) are indicated. Dotted black lines illustrate the approximate limits of frontal low density unit and the middle wedge/shelf unit of the marine continental wedge. Thin vertical line indicates the limit between CC and CD. Red triangles correspond to the volcanoes located near the profile. Pink dots correspond to slab geometry according to SLAB2.0 model (Hayes et al., 2018). Green dots depict the continental Moho depths obtained by receiver functions analysis (Dzierma et al., 2012a). Black dots indicate the base of poor compacted shallow sedimentary layer according to MT and TEM soundings and cyan dots correspond to minimum thickness of this sedimentary layer according to MT and TEM soundings.

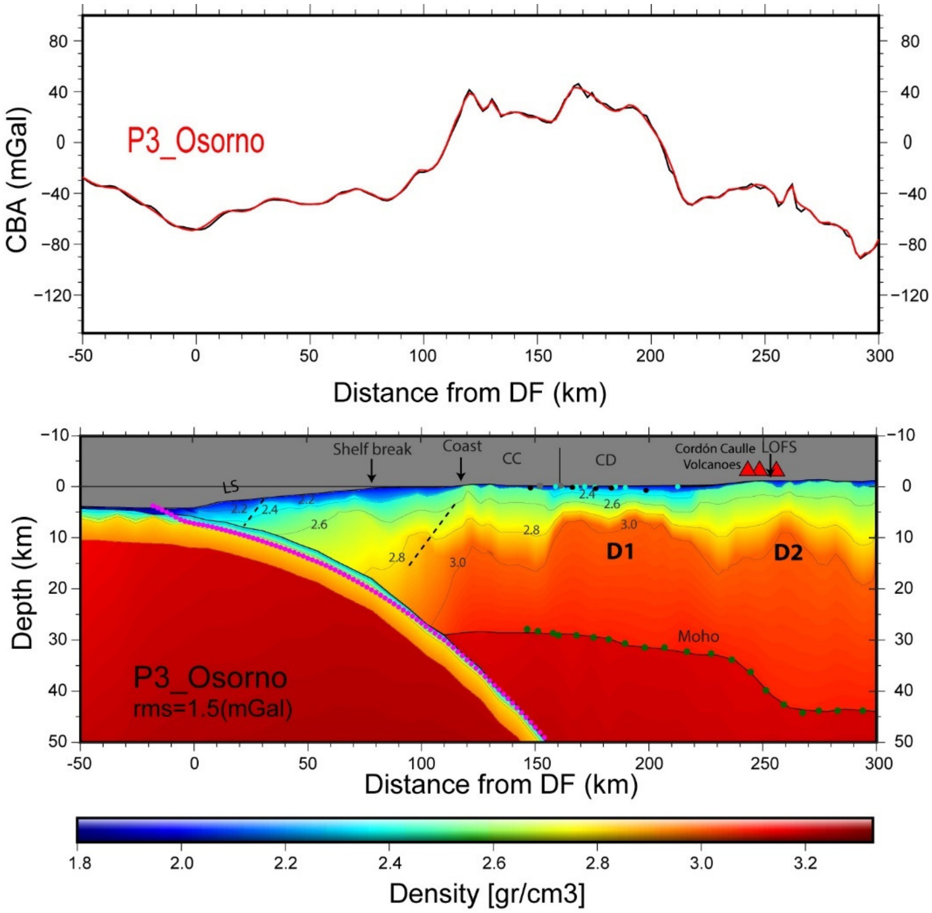

Figure S5.3: 2D regional forward model at profile P3_Osorno. Upper panel shows the observed Complete Bouguer Anomaly (CBA) in black and the calculated curve in red. Lower panel present the corresponding density depth model, morphological limits of the continental wedge (as lower slope, LS) are indicated. Dotted black lines illustrate the approximate limits of frontal low density unit and the middle wedge/shelf unit of the marine continental wedge. Thin vertical line indicates the limit between CC and CD. Red triangles correspond to the volcanoes located near the profile. Pink dots correspond to slab geometry according to SLAB2.0 model (Hayes et al., 2018). Green dots depict the continental Moho depths obtained by receiver functions analysis (Dzierma et al., 2012a). Grey dots show the base of poor compacted shallow sedimentary layer according to onshore seismic profiles and ENAP boreholes (McDonough et al., 1997; Jordan et al., 2001; Honores et al., 2015). Black dots indicate the base of poor compacted shallow sedimentary layer according to MT and TEM soundings and cyan dots correspond to minimum thickness of this sedimentary layer according to MT and TEM soundings.

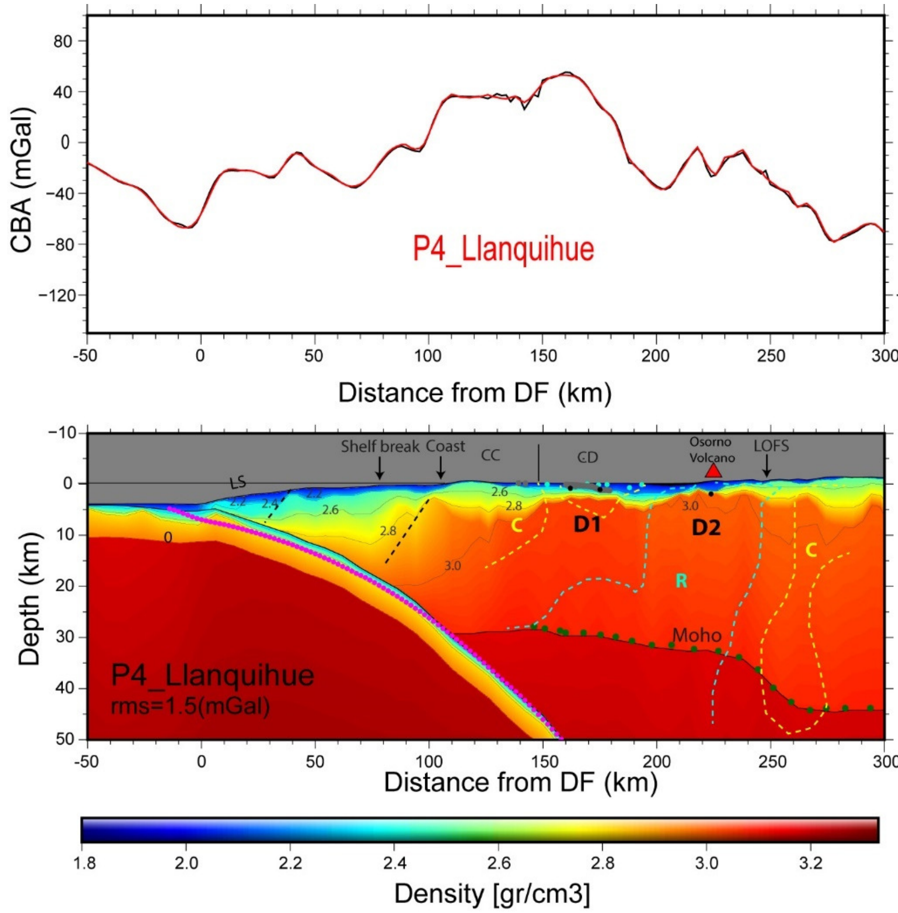

Figure S5.4: 2D regional forward model at profile P4_Llanquihue. Upper panel shows the observed Complete Bouguer Anomaly (CBA) in black and the calculated curve in red. Lower panel present the corresponding density depth model, morphological limits of the continental wedge (as lower slope, LS) are indicated. Dotted black lines illustrate the approximate limits of frontal low density unit and the middle wedge/shelf unit of the marine continental wedge. Thin vertical line indicates the limit between CC and CD. Red triangles correspond to the volcanoes located near the profile. Pink dots correspond to slab geometry according to SLAB2.0 model (Hayes et al., 2018). Green dots depict the continental Moho depths obtained by receiver functions analysis (Dzierma et al., 2012a). Grey dots show the base of poor compacted shallow sedimentary layer according to onshore seismic profiles and ENAP boreholes (McDonough et al., 1997; Jordan et al., 2001; Honores et al., 2015). Black dots indicate the base of poor compacted shallow sedimentary layer according to MT and TEM soundings and cyan dots correspond to minimum thickness of this sedimentary layer according to MT and TEM soundings. Thin dotted yellow and cyan lines limit electrical conductive and resistive zones (C and R) according to Segovia et al. (2021).

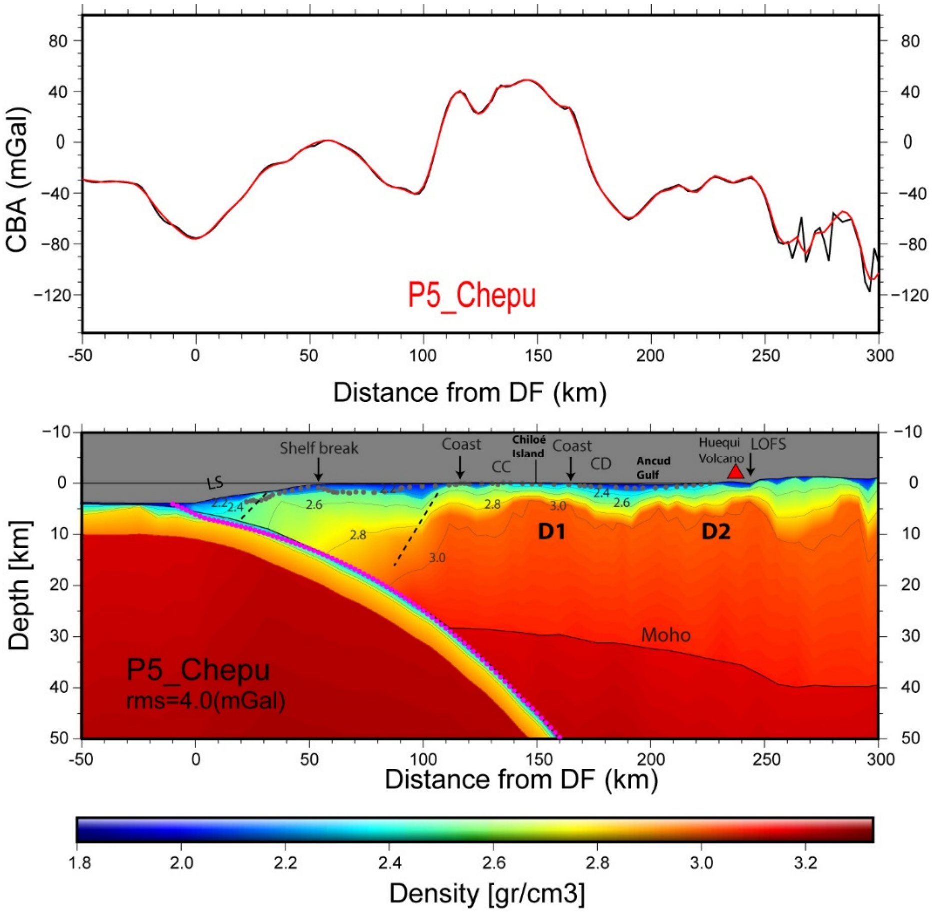

Figure S5.5: 2D regional forward model at profile P5_Chepu. Upper panel shows the observed Complete Bouguer Anomaly (CBA) in black and the calculated curve in red. Lower panel present the corresponding density depth model, morphological limits of the continental wedge (as lower slope, LS) are indicated. Dotted black lines illustrate the approximate limits of frontal low density unit and the middle wedge/shelf unit of the marine continental wedge. Thin vertical line indicates the limit between CC and CD. Red triangles correspond to the volcanoes located near the profile. Pink dots correspond to slab geometry according to SLAB2.0 model (Hayes et al., 2018). Green dots depict the continental Moho depths obtained by receiver functions analysis (Dzierma et al., 2012a). Grey dots represent the base of shallow sedimentary layers according to seismic reflection data (González, 1989).

6 Density model sensitivity to topography averaging

The method of 2D extension of the model in the direction perpendicular to profile overestimates the effect of local topographic features located exactly in the profile track. To avoid this problem, we averaged the topography (in the direction perpendicular to profile) in a 40 km-wide band (i.e., 20 km to both sides of the line). A 40 km-wide band is a reasonable assumption considering that the wavelengths of the CBA gravity anomalies along the profiles are mostly larger than ~40-50 km as is showed in the amplitude spectrum (see figure S6.1). Then, this scale is reasonable option to represent regional features in the direction perpendicular to the profiles. On the other hand, this parameter is not critical for the obtained 2D model. In fact, a completely different value (10 km-wide, i.e. 5 km to both sides of the line) can be considered with minor modification in the resulting density model (and similar rms between observed and modeled data), which indicates that this “wide” is not a critical value for our modelling scale (see figure S6.2).

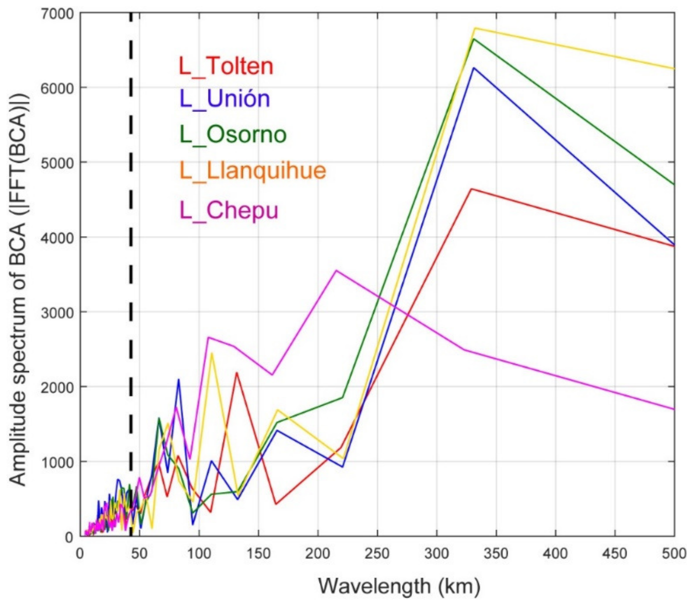

Figure S6.1: Amplitude spectrum of BCA signal along the 5 gravity profiles used to generate 2D forward models. Dotted vertical line highlights the wavelength equal to 40 km.

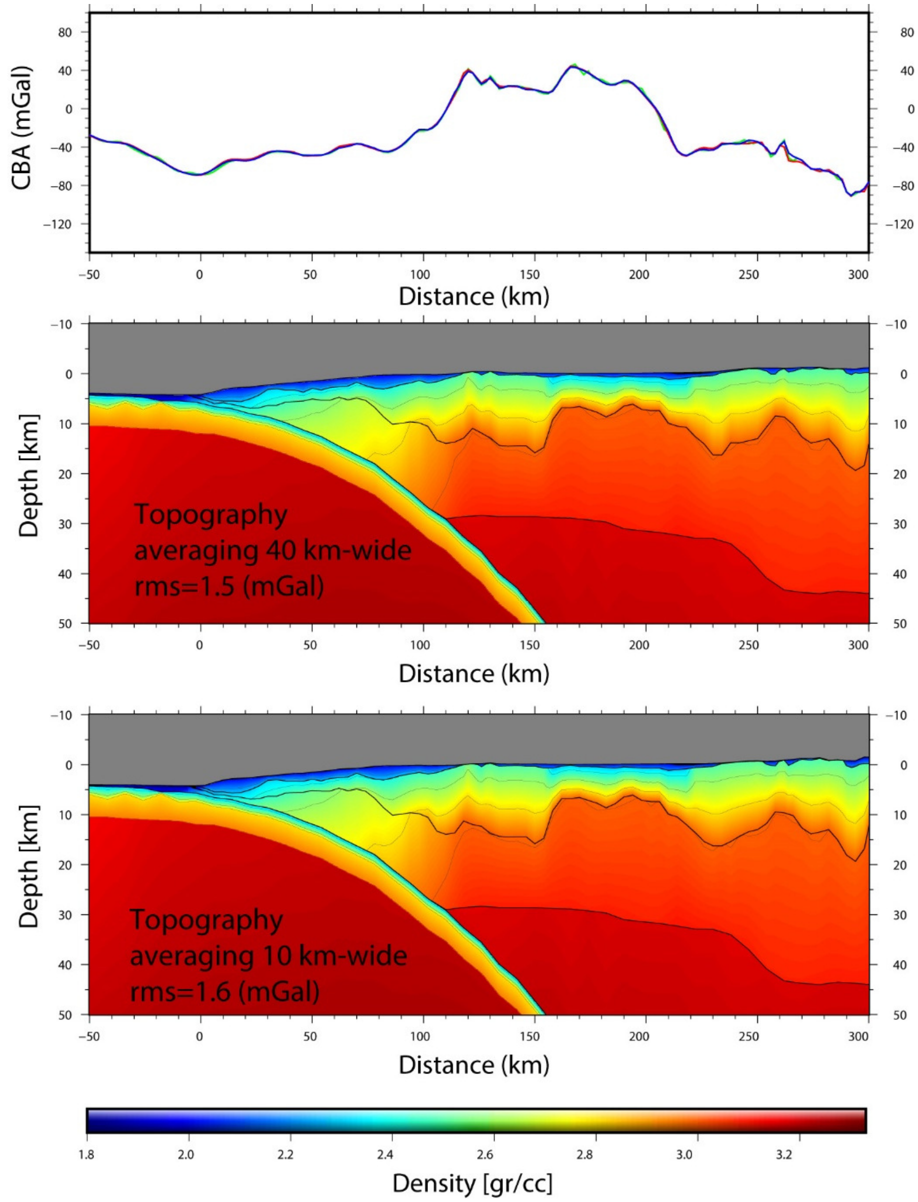

Figure S6.2: Comparison between 2D forward models obtained with different bands of topography-averaging in the Osorno profile. Central panel corresponds to model obtained with a band 40km-wide of topography averaging (corresponding modeled gravity is presented in blue at the upper panel). Lower panel corresponds to model obtained with a band 10km-wide of topography averaging (corresponding modeled gravity is presented in red at the upper panel. Observed data corresponds to green line in the upper panel).

S7 Regional gravity trend

In order to generate the Residual Bouguer Anomaly used as input data to the 3D local inversion, a 1th order polynomial trend was subtracted from the Complete Bouguer Anomaly data. The equation of the fitted linear trend (in mGal) is:

$$REG(x,y) = -3.12000000000019 - 0.000569517021292329\,(x - 666000) - 0.0000030685267071916\,3 *(y-5448000)$$

were x and y are UTM-East and UTM-north coordinates, respectively (datum WGS84-18S).

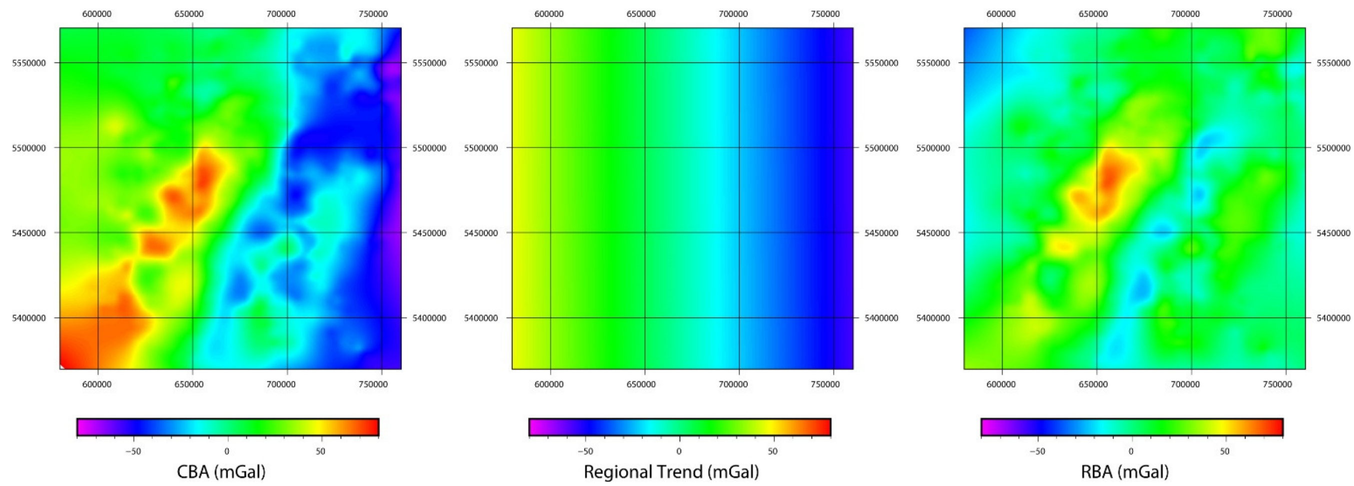

Figure S7.1: Complete Bouguer Anomaly (CBA), Linear Regional trend and Residual Bouguer Anomaly (RBA).

S8 3D cuts through the inverted density model

The figure S7.1 shows 3D cuts through the inverted density model at several UTM-North coordinates and reaching 44 km depth. As is observed the solution is almost homogeneous below ~20 km depth, which suggest that the linear regional trend removed from Complete Bouguer Anomaly to generate the Residual Bouguer (i.e., the input data) is a reasonable representation of the long wavelength gravity signal generated by deeper density structure of the crust and mantle.

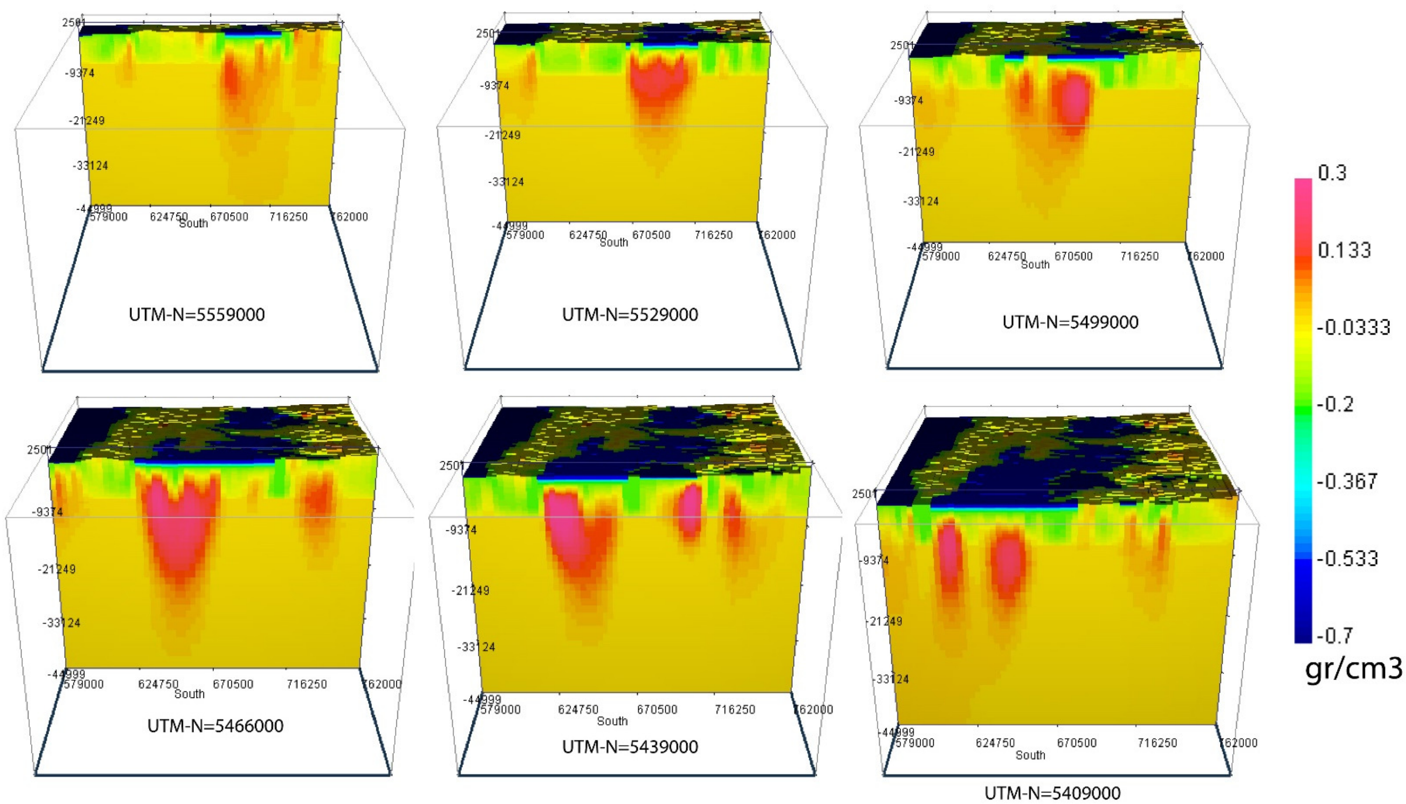

Figure S8.1: 3D cuts through the inverted density model at several UTM-North coordinates (5559000, 552900, 5499000, 5466000, 5439000, 5409000).

9 Sensitivity of 3D density inversion

As any gravity modeling, the 3D density inversion presents not uniqueness in the solution, which is an important methodological reason to use independent model methodologies (2D forward and 3D inversion, in this case) and independent geophysical/geological information to constrains the result. However, several inversions were run to study the sensitivity of the solution under the variation of selected parameters or input data. In UBC-GIF software, length scale parameters (L_E, L_N, L_Z) define the horizontal and vertical smoothness of the solution (https://www.eoas.ubc.ca/ubcgif/iag/index.htm). We preferred values of L_E =6000 m, L_N =6000 m and L_z =3000 m, which is the double of the horizontal and vertical cell size (maximum vertical cell size=1500 m) used to discretize the media. This criterion is one of the recommended in the software manual (https://www.eoas.ubc.ca/ubcgif/iag/index.htm), but also it is important to highlight that under a strong variation these parameters, the obtained solution of density structure shows similar features (see Figure S8.1 and Figure S8.2)

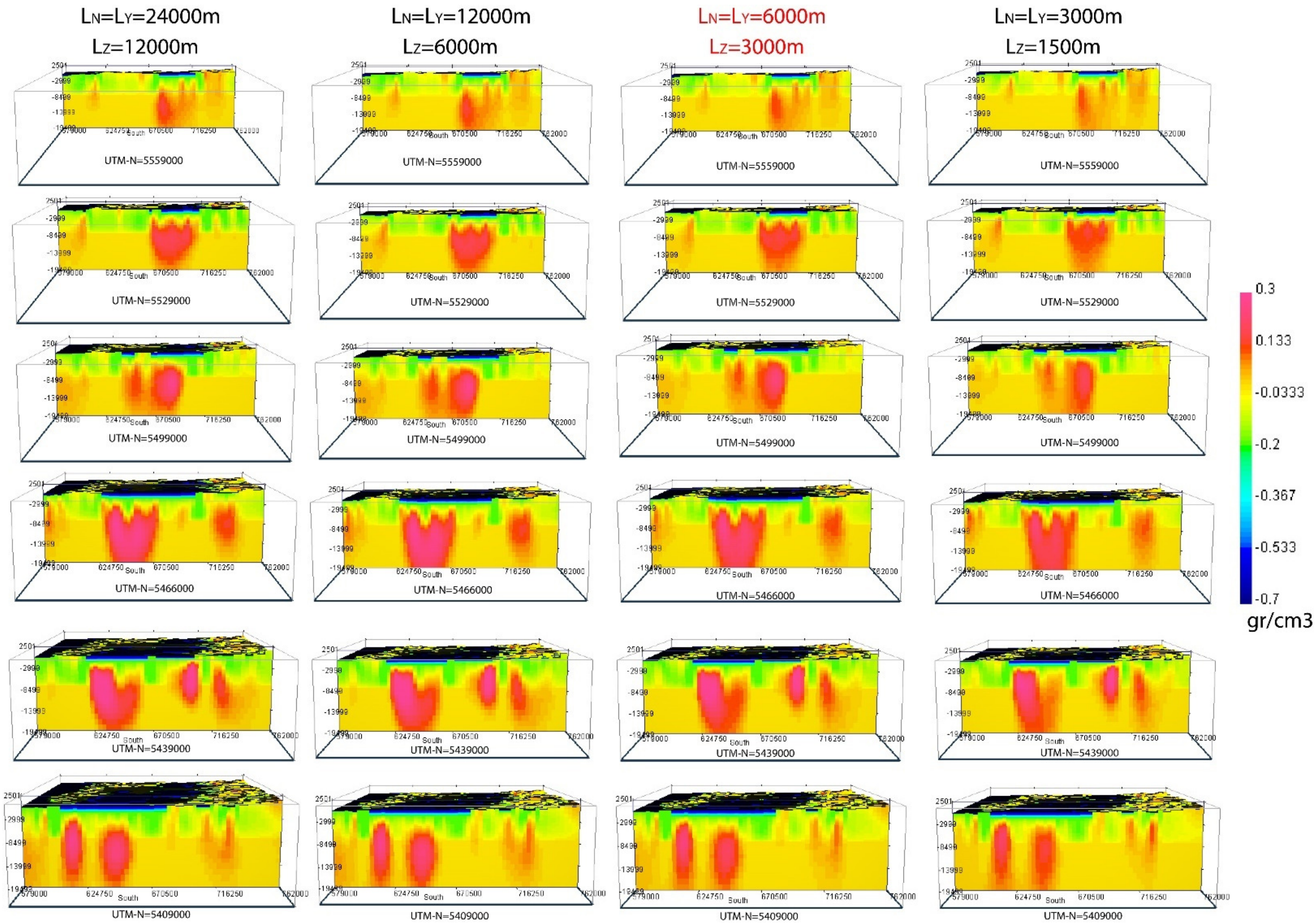

Figure S9.1: 3D density structure obtained for different length scale parameters (L_N, L_E, L_Z) of the UBC-GIF algorithm. Each column presents 3D cuts at six constant UTM-North coordinates (5559000, 552900, 5499000, 5466000, 5439000, 5409000). Third column corresponds to model presented in the main text.

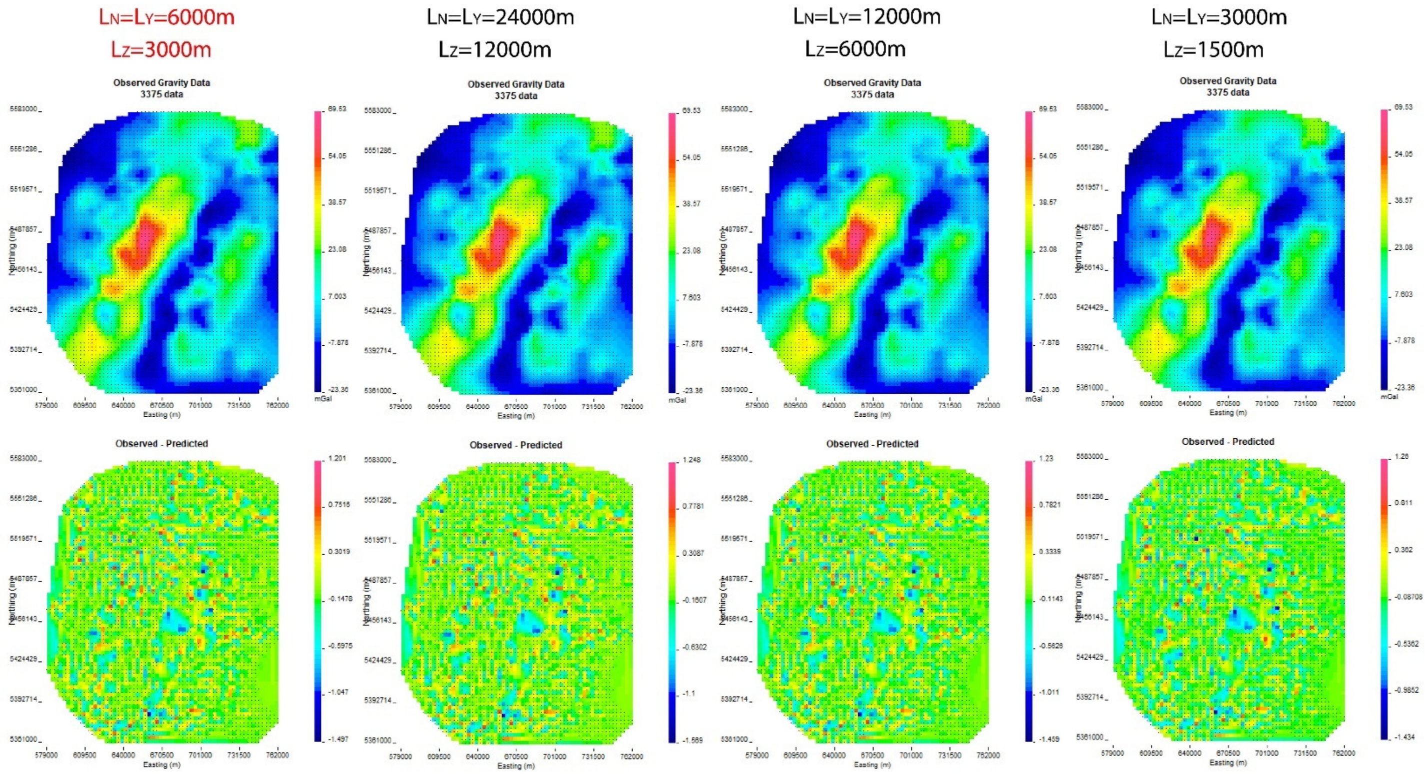

Figure S9.2: Difference between input gravity data (observed data) and modeled gravity (predicted) associated to 3D models obtained by different length scale parameters (see previous figure for corresponding density models). Upper panel, in each column, presents a grid of input gravity data (observed data) and the lower panel shows a grid of the difference between observed and predicted data in mGal. First column corresponds to model presented in the main text.

In order to show the stability of the solution under variation of input data, we modified the observed gravity by adding random noise with different amplitude and also a numerical artifact generated by a sinusoidal function with different wavelengths. Figure S8.3 shows examples of inversion generated after adding random noise to original input data. i.e:

(s1) Input gravity data = original gravity data ± Random noise

Random noise corresponds to aleatory numbers added to input data (different at each point of input gravity grid) which can take values between 0 and certain amplitude. In the examples presented in the figures S8.3 and S8.4 the random noise can reach values of 1, 2.5 and 5 mGal. As is observed, the main characteristics of the original solution are also obtained with the modified input data, even considering a maximin random noise of 5 mGal.

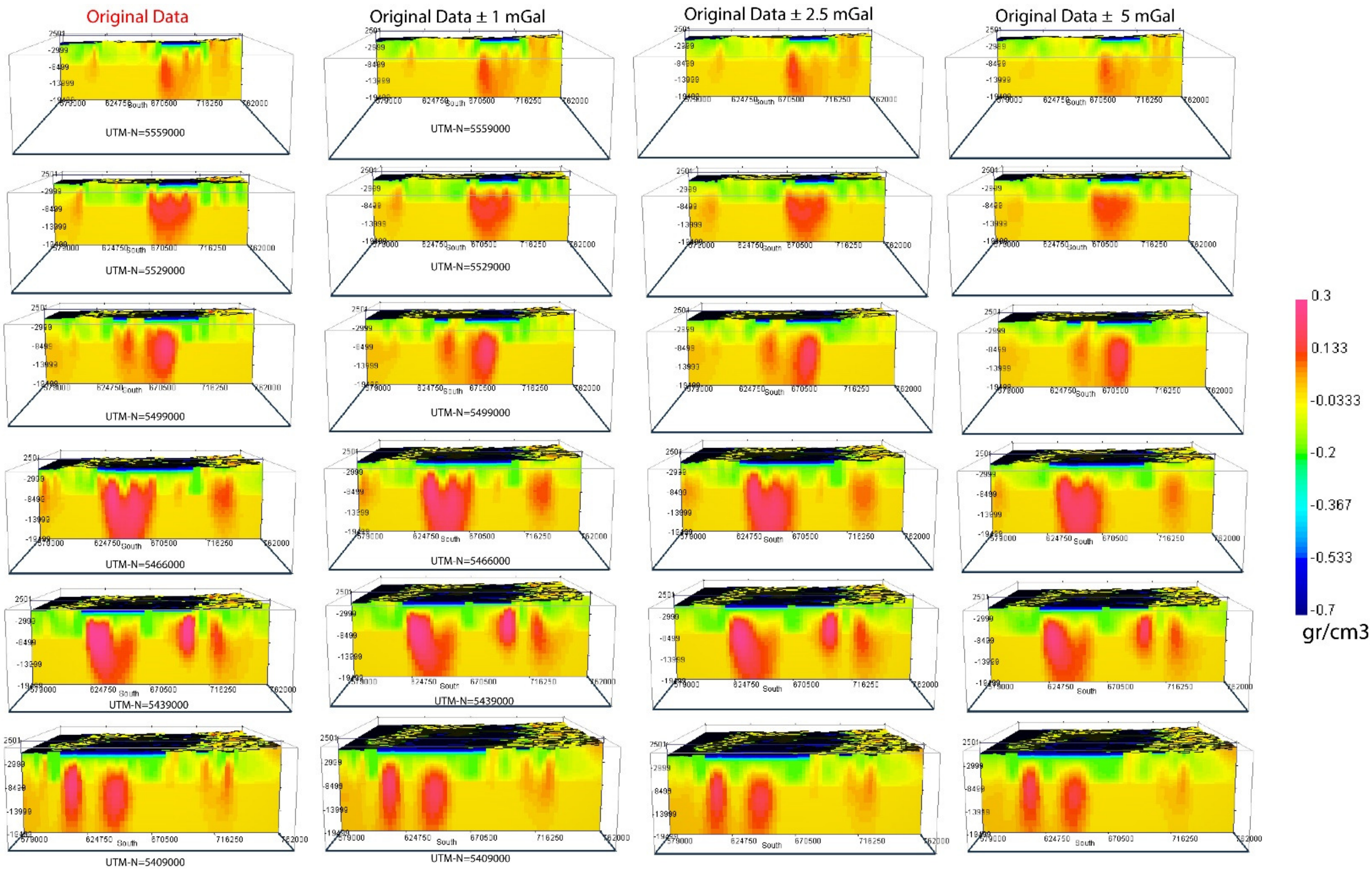

Figure S9.3: 3D density structure obtained for different maximum amplitude of the random noise. Each column presents 3D cuts at six constant UTM-North coordinates (5559000, 552900, 5499000, 5466000, 5439000, 5409000). First column corresponds to the model presented in the main text. Other models result after the introduction of random noise to the original data with maximum amplitude of 1, 2.5, and 5 mGal.

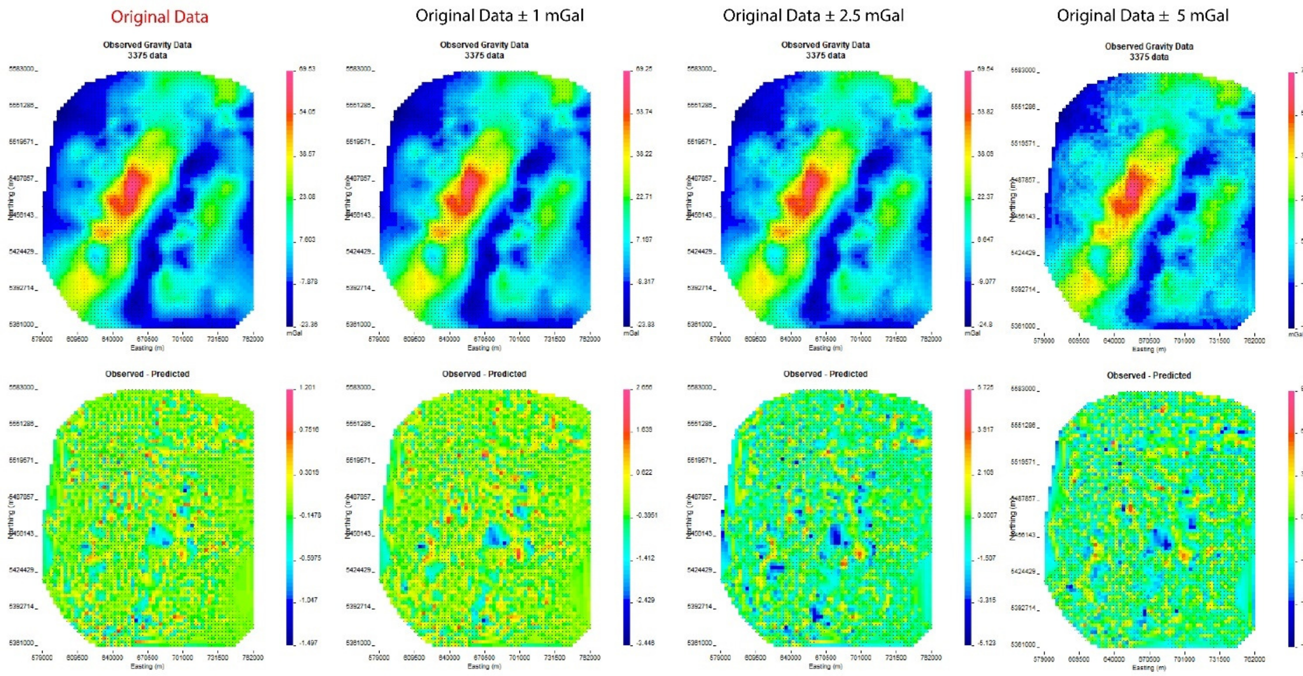

Figure S9.4: Difference between input gravity data (observed data) and modeled gravity (predicted) associated to 3D models obtained by different maximum amplitude of the random noise (see previous figure for corresponding density models). Upper panel, in each column, presents a grid of input gravity data (observed data) and the lower panel shows a grid of the difference between observed and predicted data in mGal. First column corresponds to model presented in the main text.

Similar results are obtained by adding artifacts of large wavelength and amplitude. To show this, we add a sinusoidal function and a constant gravity value, i.e.:

$$\text{Input gravity data} = \text{original gravity data} + A\left(\cos(\pi (X-X0)/B) + \cos(\pi (Y-Y0)/B) - 1\right) \qquad \text{(s2)}$$

Were X, Y are the UTM coordinates of the original gravity data, X0 and Y0 are the minimum Eastern and Northern coordinates of the original gravity data. The parameter A controls the amplitude of the sinusoidal function and constant gravity artifact, and B corresponds to the wavelength of the sinusoidal function. Figures S8.5 and S8.6 shows the results of this experiment for different values of A and B parameters. It is interesting to observe that, even under a strong modification of the input data (e.g., A=10, B=10km in Figure S8.6), the resulting density structure is different from the obtained by the real (original) data but the wavelength of the main anomalies and its position is preserved (Figure S8.5).

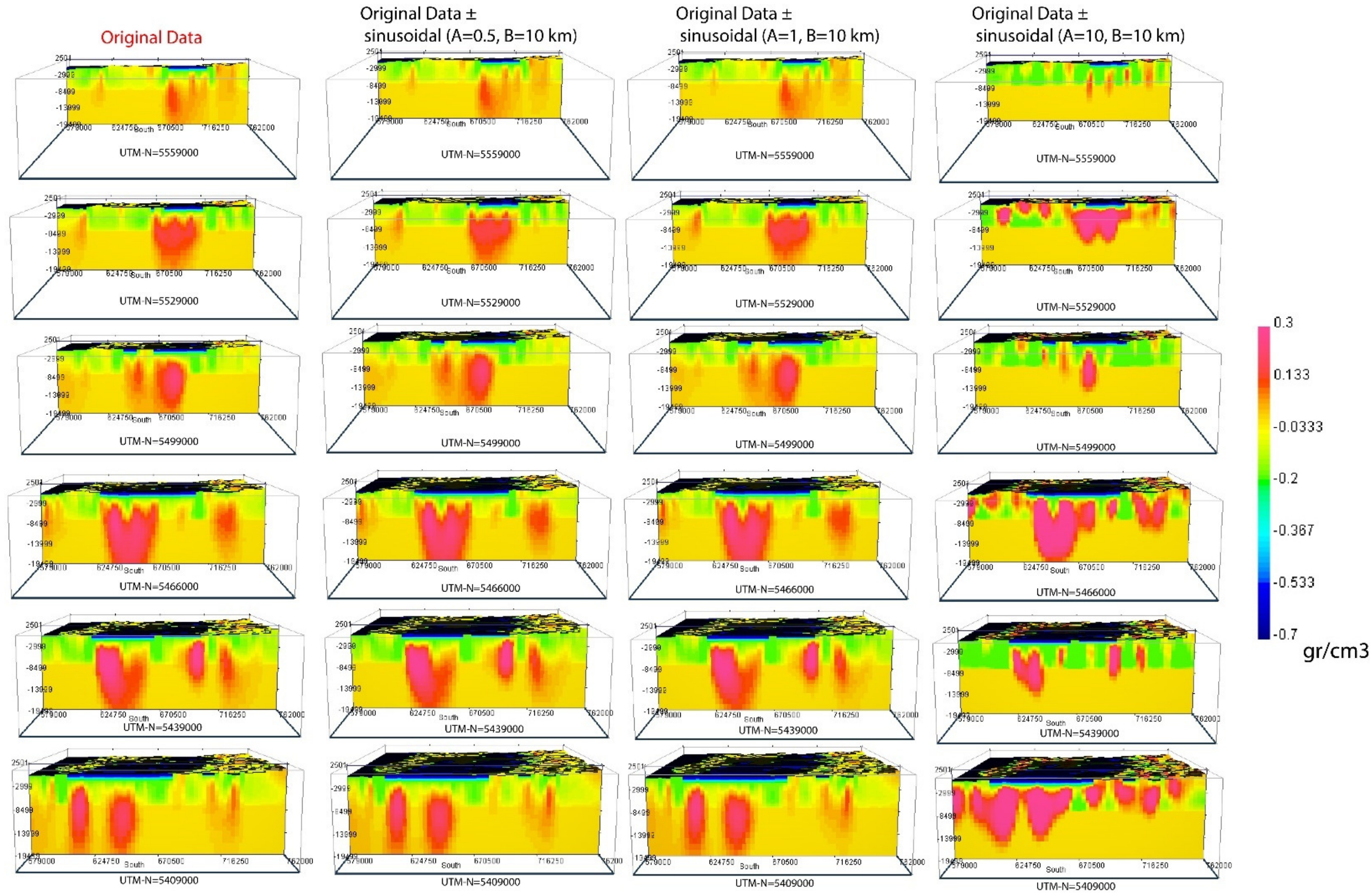

Figure S9.5: 3D density structure obtained for modified input data by adding sinusoidal and constant gravity artifacts. Each column presents 3D cuts at six constant UTM-North coordinates (5559000, 552900, 5499000, 5466000, 5439000, 5409000). First column corresponds to the model presented in the main text. Other models result after adding function (s2) with different values of parameters A and B.

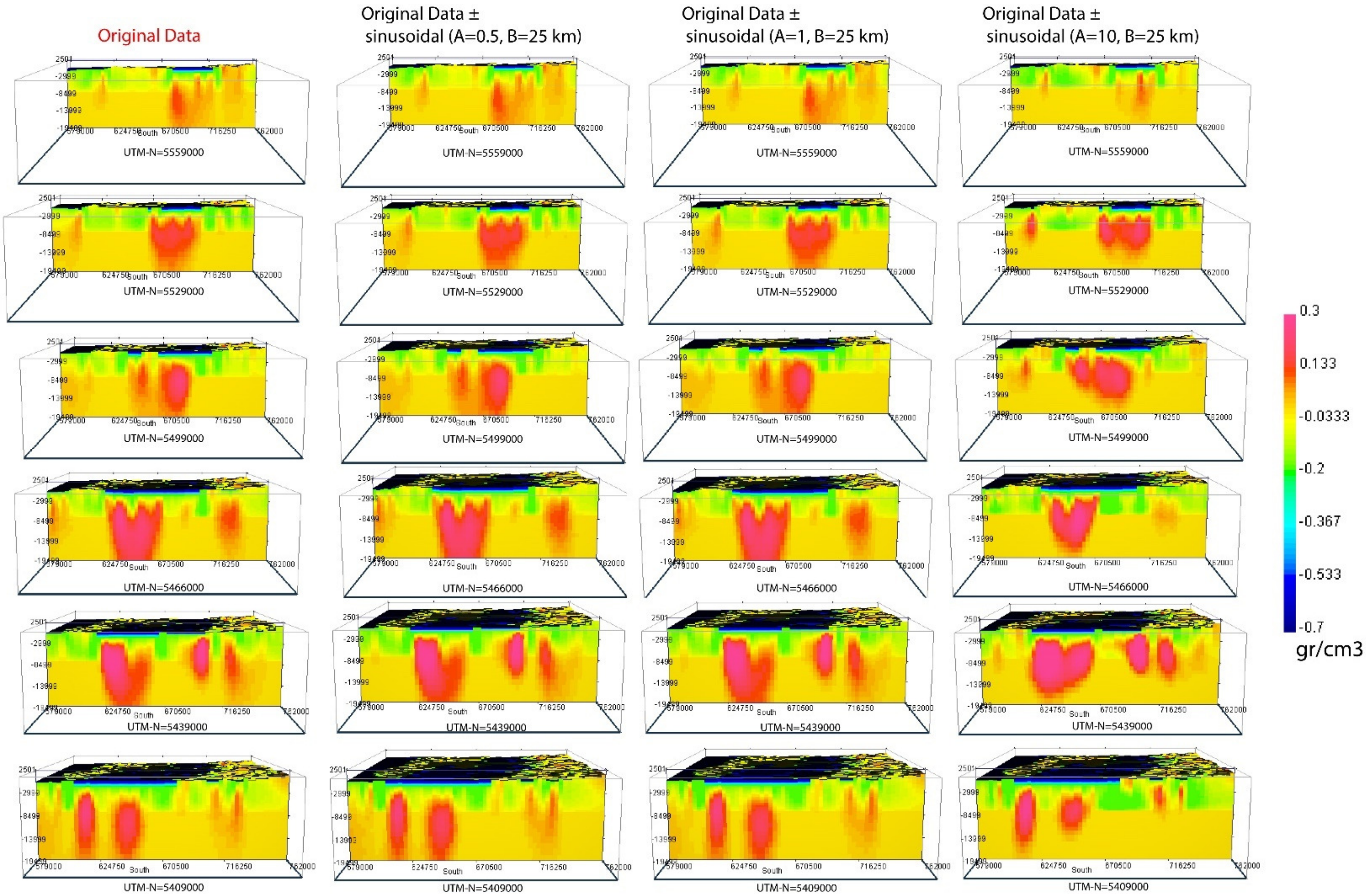

Figure S9.5: continued

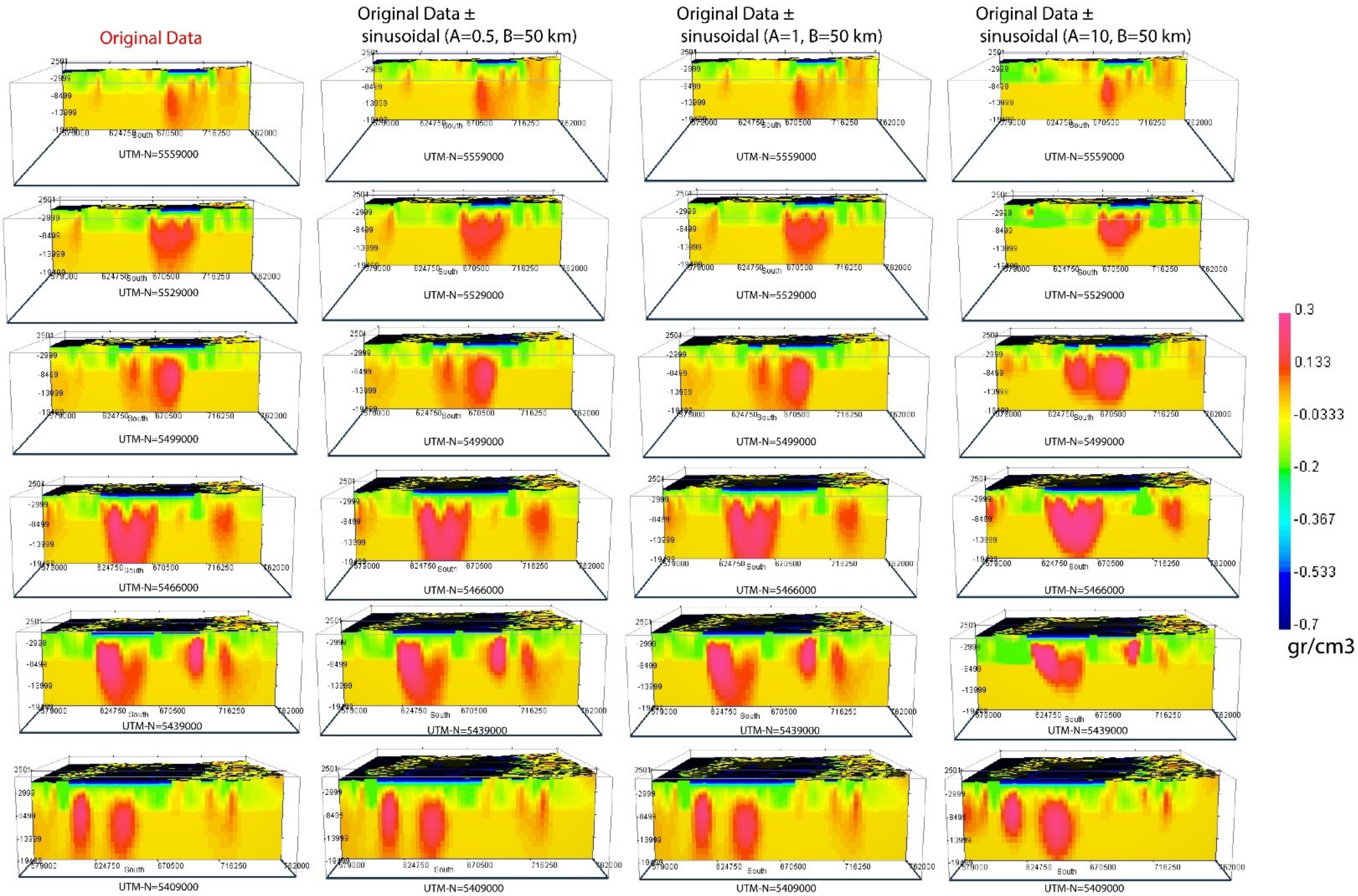

Figure S9.5: continued

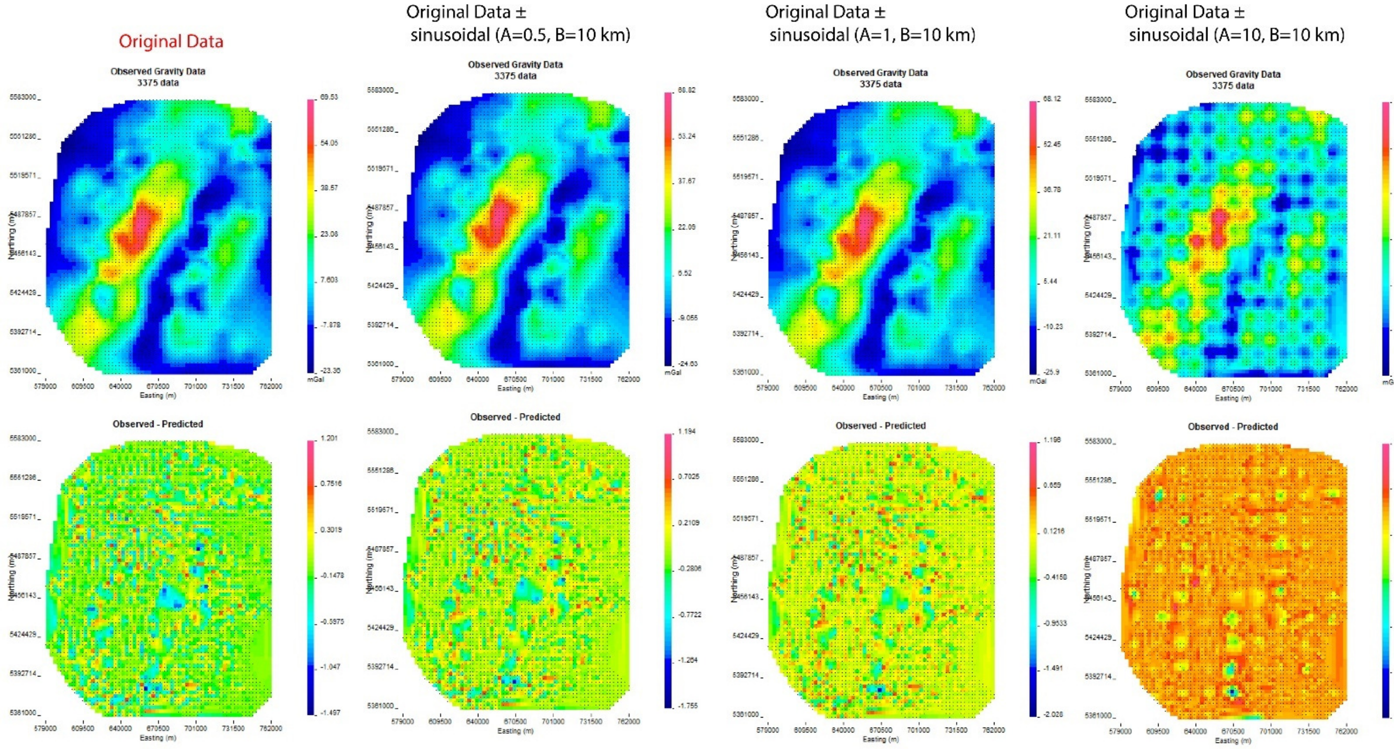

Figure S9.6: Difference between input gravity data (observed data) and modeled gravity (predicted) associated to 3D models obtained input data with the addition of sinusoidal and constant gravity artifacts (see previous figure for corresponding density models). Upper panel, in each column, presents a grid of input gravity data (observed data) and the lower panel shows a grid of the difference between observed and predicted data in mGal. First column corresponds to model presented in the main text.

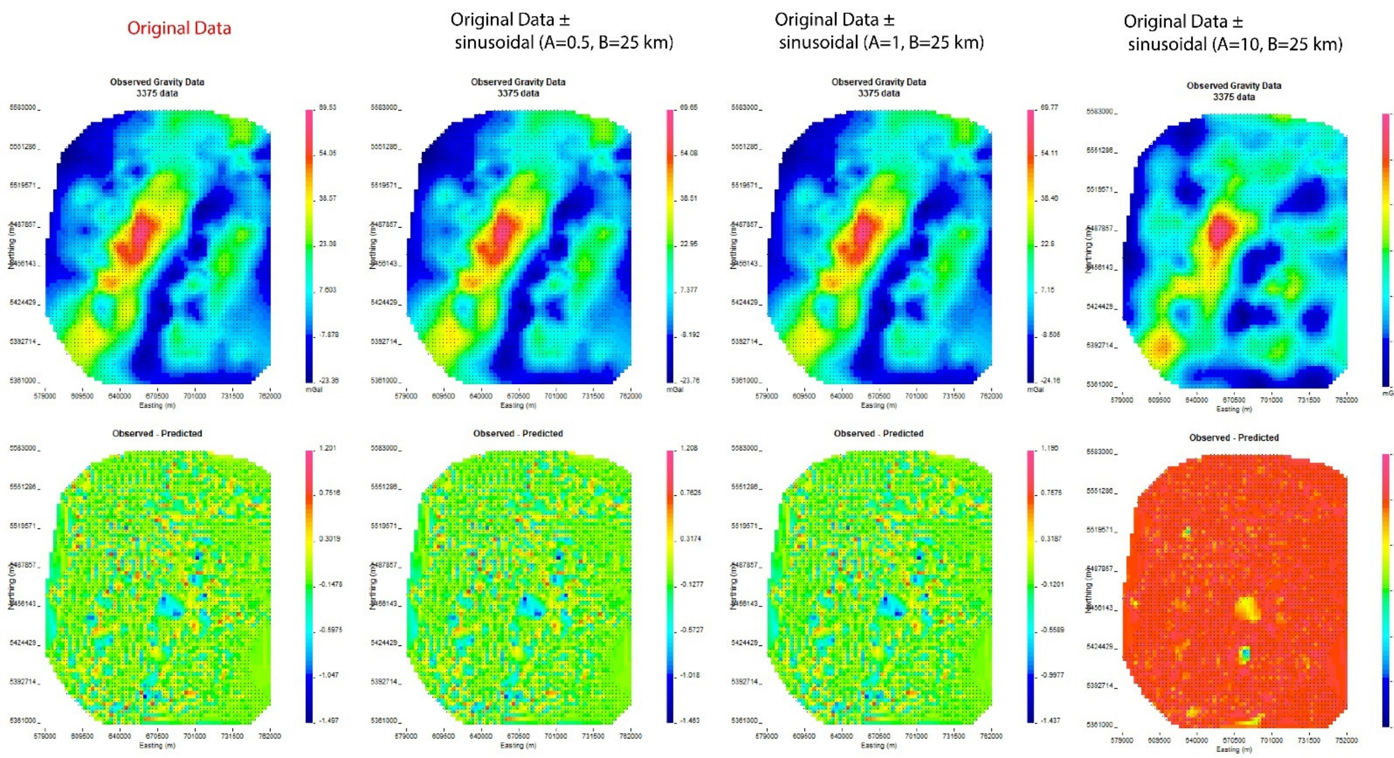

Figure S9.6: continued

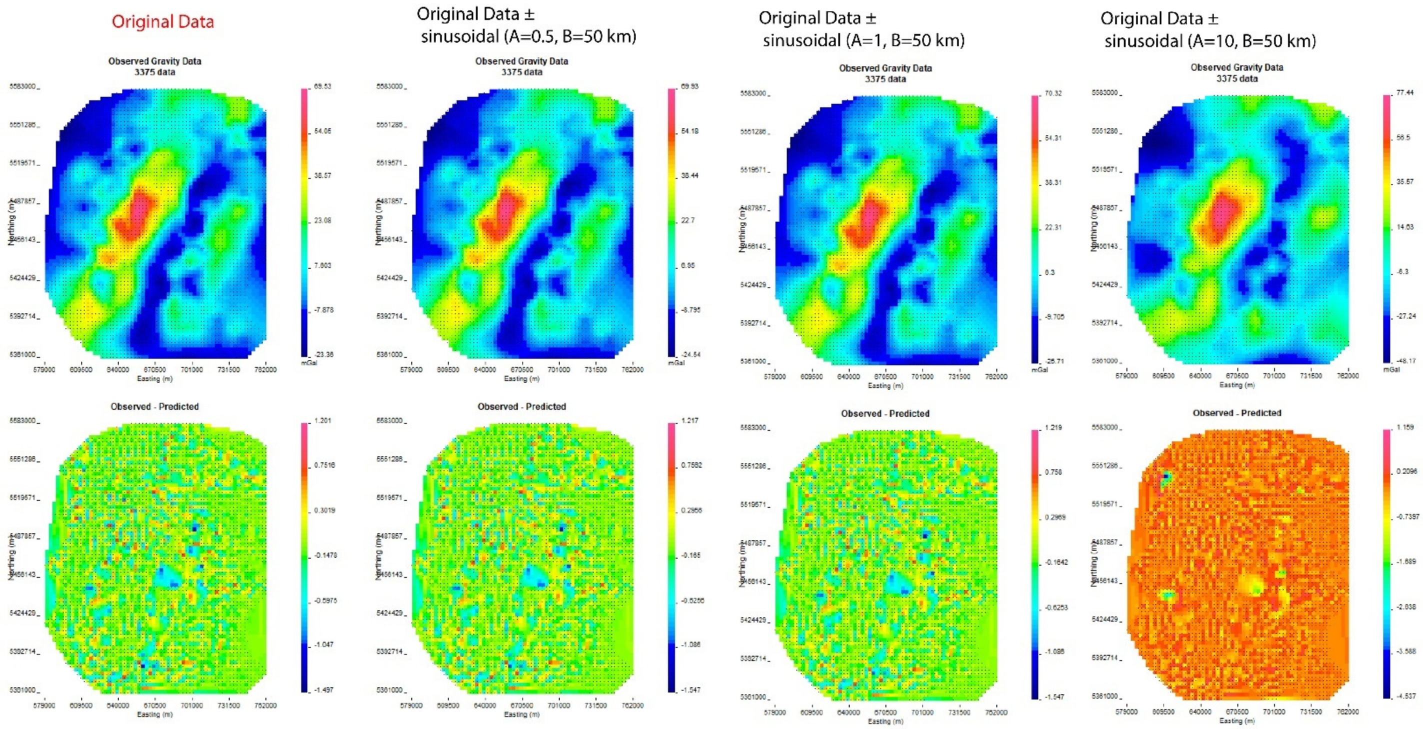

Figure S9.6: continued